Filomat 39:18 (2025), 6185–6198
https://doi.org/10.2298/FIL2518185N

Published by Faculty of Sciences and Mathematics,
University of Niš, Serbia
Available at: http://www.pmf.ni.ac.rs/filomat

# Numerical investigation of SIR epidemic model using Fibonacci wavelets

**Naied A. Nayied[a], Firdous A. Shah[b,*], Mukhtar A. Khanday[a]**

[a] *Department of Mathematics, University of Kashmir, Srinagar 190006, Jammu and Kashmir, India*
[b] *Department of Mathematics*
*University of Kashmir, South Campus, Anantnag 192101, Jammu and Kashmir, India*

**Abstract.** The susceptible-infected-recovered (SIR) epidemic model consists of a system of non-linear ordinary differential equations that model the spread of non-fatal disease in the human population. In this article, the Fibonacci wavelet-based collocation method is proposed for solving the SIR epidemic model. The proposed scheme starts with the construction of operational matrices of integration based on Fibonacci wavelets. Operational matrices of integration are then employed to convert the given SIR epidemic model into a system of algebraic equations. Moreover, the Jacobian technique is utilized to linearize the given non-linear model. Furthermore, the obtained results of the SIR epidemic model are then compared with other existing numerical methods, including the fourth-order Runge-Kutta and residual power series methods. At the end, the numerical simulations for the susceptible, infected, and recovered populations are carried out via graphs and tables.

## 1. Introduction

Epidemiology is one of the most popular research areas in the field of biological sciences, which describes the spread of infectious diseases on a larger scale in a particular area of a given population. In particular, it plays an important role for better understanding of infectious diseases in a defined population. Generally, infectious diseases are caused by pathogenic organisms that infect a host organism and can spread from one organism to another organism either directly or indirectly. Infectious diseases regularly affect a significant number of populations across a vast geographical area and have thus attracted biologists and mathematicians to carry out significant research on the mathematical models describing infectious diseases. Among the most prevalent infectious diseases include whooping cough [1], influenza [2], rubella [3], measles [4], tuberculosis [5] and many more.

In the current study, the entire population involved in the transition of infection is categorized into three epidemiological classes: a susceptible class (S), an infected class (I), and a removed class (R), which stands for persons who have been immunized and have recovered with permanent immunity from the disease. The susceptible-infected-recovered (SIR) epidemic model was first introduced by Kermack and

2020 *Mathematics Subject Classification*. Primary 65T60; Secondary 34A34, 92D30.
*Keywords*. SIR epidemic model; Fibonacci wavelet method; Haar wavelet method; Operational matrix.
Received: 29 April 2024; Revised: 11 April 2025; Accepted: 23 June 2025
Communicated by Hari M. Srivastava
* Corresponding author: Firdous A. Shah
*Email addresses:* naiedahmad12@gmail.com (Naied A. Nayied), fashah@uok.edu.in (Firdous A. Shah), khanday@uok.edu.in (Mukhtar A. Khanday)

McKendrick [6] in the 19th century in order to understand the dynamic behavior of infectious diseases. It is one of the most basic compartmental models in epidemiology. There are several articles in the literature that investigate the transmission dynamics of viruses and are derived from the basic SIR model. For instance, the SIR epidemic model has been employed to investigate epidemiological phenomena including the spread of smallpox [7], influenza [8], and HIV [9]. Many researchers developed mathematical models to describe the coronavirus pandemic's circumstances. Mathematical modeling plays an important role in gaining a better understanding of disease transmission and provides many techniques for preventing the spread of disease. The SIR epidemic model is characterized by the following first-order system of non-linear differential equations:

$$\left.\begin{aligned} \frac{dS}{dt} &= -\alpha SI \\ \frac{dI}{dt} &= \alpha SI - \beta I \\ \frac{dR}{dt} &= \beta I \end{aligned}\right\}, \tag{1}$$

with initial conditions $S(0) = S_0, I(0) = I_0, R(0) = R_0$ and is assumed that the total population remains constant $N$, that is; $S(t) + I(t) + R(t) = N$. The SIR model consists of three compartments:

- $S(t)$ is the number of individuals in the susceptible compartment, all individuals in this group are susceptible if they contract the disease and are immune of being infected at time $t$.
- $I(t)$ is the number of individuals in the infected compartment, all individuals in this group are infected by the disease and can transmit it to the susceptible individuals at a time $t$.
- $R(t)$ is the number of individuals in the removed (recovered or dead) compartment, in this group, either an individual has recovered from disease or has died due to disease at time $t$.
- $\alpha$ represents the population's rate of transition from susceptible to infected.
- $\beta$ represents the transition rate from infected to immune(permanent) population.

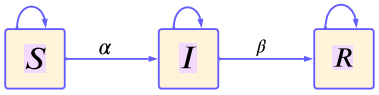


Figure 1: Flowchart representation of the basic compartmental SIR epidemic model.

During the culminating years of 19th century, wavelet theory and its ramifications have proven to be of utmost significance due to its various applications in science and engineering fields, including digital signal and image processing, pattern recognition, quantum physics, and many more. Wavelets obey certain elegant properties such as orthogonality, compact support, and good localization, which has attracted a wider class of researchers to investigate and study diverse areas related to various wavelet-based numerical methods [10, 11]. Wavelet-based collocation methods have achieved significant recognition in numerical analysis, due to their straightforward implementation, efficient computation, and rapid convergence. Additionally, these methods are particularly advantageous for computer-based applications, as they don't require computing the inverse wavelet matrices, thereby reducing CPU time requirements. It is noteworthy that researchers have obtained the numerical solution to a wide range of both linear and non-linear differential equations by using wavelet-based methods, including the Haar wavelets, Chebyshev wavelets, Legendre wavelets, Gegenbauer wavelets, and Fibonacci wavelets [12–15].

Keeping in view the pleasant characteristics of the Fibonacci wavelets, such as regularity, higher degree of smoothness and compact support, the main aim of this article is to develop an efficient numerical

technique based on Fibonacci wavelets for obtaining the numerical solution of the SIR epidemic model (1). The motivation and philosophy behind this approach is that it converts the given model into a system of algebraic equations that can be solved conveniently by any classical method such as Newton's iterative method. The operational matrices of integration based on Fibonacci and Haar wavelets are obtained by using the machinery of Chen and Hsiao [16]. The operational matrices of integration are then utilized to convert the given system of non-linear differential equations into a system of algebraic equations.

The remainder of the article is organized as follows: In Section 2, the Fibonacci wavelets and their basic properties are introduced along with their operational matrices of integration that convert the SIR epidemic model into a system of algebraic equations. The implementation of the wavelet collocation methods on the proposed SIR epidemic model is presented in Section 3. Section 4 is the centerpiece of the article that presents the numerical simulation and discussion of the SIR model by the proposed methods. Finally, a conclusion is drawn in Section 5.

## 2. Wavelets and Function Approximation

In 1982, Jean Morlet first introduced the idea of wavelets as a family of functions obtained from dilation and translations of a single function called *mother wavelet*. The formal definition of a mother wavelet is characterized by the notion of *admissibility*, which allows the reconstruction of the input signal from the transformed one. A function $\psi \in L^2(\mathbb{R})$ is said to be an admissible wavelet if the following condition holds:

$$C_\psi = 2\pi \int_{\mathbb{R}} \frac{\left|\hat{\psi}(\omega)\right|^2}{|\omega|}\, d\omega < \infty. \tag{2}$$

The condition given by equation (2) is referred to as *admissibility condition*. From From this equation, we deduce that $\hat{\psi}(\omega) \to 0$ as $\omega \to 0$. Specifically, if $\hat{\psi}(\omega)$ is continuous, then $\hat{\psi}(0) = 0$; that is, $\int_{\mathbb{R}} \psi(t)\, dt = 0$, which implies that $\psi$ must be an oscillatory function with zero mean. Consequently, a wavelet $\psi$ is is inherently an oscillating function, and in fact should have good time localization properties so that it looks like a *small wave*. That is why $\psi$ is named as a *wavelet*. In addition to the admissibility condition, other properties become relevant in specific applications. For instance, restrictions on the support of $\psi$ and its Fourier transform $\hat{\psi}$ or the requirement for $\psi$ to have a certain number of vanishing moments that represent the regularity of the wavelet functions to capture localized information. A wavelet $\psi(t)$ is said to have $n$-vanishing moments if it satisfies the following condition:

$$m_k = \int_{\mathbb{R}} t^k \psi(t)\, dt = 0, \quad k = 0, 1, \ldots, n. \tag{3}$$

This property reflects the regularity of the wavelet functions and their ability to capture localized features. Applying the translation and scaling operators to a mother wavelet $\psi(t)$ gives rise to a family of *daughter wavelets* as

$$\psi_{a,b}(t) = |a|^{-1/2} \psi\left(\frac{t-b}{a}\right), \tag{4}$$

where $a \in \mathbb{R}^+$ and $b \in \mathbb{R}$ are the scaling and translation parameters. The scaling parameter quantifies the level of compression or scale, while the translation parameter $b$ specifies the temporal position of the wavelet. For $0 < a < 1$, the wavelet $\psi_{a,b}(t)$ given by (4) is the compressed version, while for $a > 1$ it turns to be relaxed version of the mother wavelet $\psi(t)$. Typical example of a wavelet is the Haar wavelet, which is in fact the simplest and oldest orthonormal wavelet with compact support. Other examples of prominent wavelets include the Morlet, Mayer, Shannon, Mexican hat and Fibonacci wavelets [17].

In the sequel, we aim to construct the operational matrices of integration based on Fibonacci and Haar wavelets for obtaining the numerical solution of the SIR epidemic model. To begin with, we present an overview of the fundamental notion of wavelets

*2.1. Fibonacci Wavelets and Function Approximation*

This subsection is proposed for the construction of Fibonacci wavelets by utilizing the Fibonacci Polynomials. For any $t \in \mathbb{R}^+$, the Fibonacci are recursively defined by:

$$F_{m+2}(t) = tF_{m+1}(t) + F_m(t), \tag{5}$$

with $F_0(t) = 0$ and $F_1(t) = 1$. Equivalently, the Fibonacci polynomials can be defined in closed form as:

$$F_{m-1}(t) = \frac{\lambda^m - \mu^m}{\lambda - \mu}, \qquad m \geq 1, \tag{6}$$

where $\lambda$ and $\mu$ are the roots of the companion polynomial $\eta^2 - t\eta - 1$ of the recursion. Moreover, they can be slo represented in the power form as [18]:

$$F_m(t) = \sum_{i=0}^{\lfloor m/2 \rfloor} \binom{m-i}{i} t^{m-2i}, \quad m \geq 0. \tag{7}$$

The Fibonacci wavelets on the interval $[0, 1]$ are defined by [19]:

$$\psi_{n,m}(t) = \begin{cases} \frac{2^{(k-1)/2}}{\sqrt{W_m}} F_m\left(2^{k-1}t - n + 1\right), & \left(\frac{n-1}{2^{k-1}} \leq t < \frac{n}{2^{k-1}}\right) \\ 0, & \text{otherwise,} \end{cases} \tag{8}$$

where $k$ and $n$ represent the resolution and translation parameters respectively, with $k = 1, 2, \ldots$, $n = 1, 2, \ldots, 2^{k-1}$. In equation (8), $F_m(t)$ denotes the $m^{th}$ degree Fibonacci polynomial that can be calculated by using equation (7). The factor $1/\sqrt{W_m}$ appearing in (8) is the normalization coefficient and can be computed as:

$$\begin{aligned} W_m &= \int_0^1 F_m(t) F_m(t)\, dt, \quad m = 0, 1, \ldots, M-1. \\ &= \sum_{i=0}^{\lfloor m/2 \rfloor} \sum_{j=0}^{\lfloor m/2 \rfloor} \binom{m-i}{i} \binom{m-j}{j} \left(2(-i-j) + n + m + 1\right)^{-1}. \end{aligned} \tag{9}$$

For instance, if we choose $k = 2, M = 3$, the following Fibonacci wavelet family is obtained:

$$\left.\begin{array}{ll} \left.\begin{array}{l} \psi_{1,0}(t) = \sqrt{2}, \\ \psi_{1,1}(t) = 2\sqrt{6}\, t, \\ \psi_{1,2}(t) = \sqrt{\frac{15}{14}}\,(1 + 4t^2), \end{array}\right\} & x \in \left[0, \frac{1}{2}\right) \\ \left.\begin{array}{l} \psi_{2,0}(t) = \sqrt{2}, \\ \psi_{2,1}(t) = \sqrt{6}\,(2t - 1), \\ \psi_{2,2}(t) = \sqrt{\frac{30}{7}}\left(2t^2 - 2t + 1\right) \end{array}\right\} & x \in \left[\frac{1}{2}, 1\right) \end{array}\right\}. \tag{10}$$

Any square integrable function $g(t)$ can be expanded in terms of Fibonacci wavelets as:

$$g(t) \approx g_{k,M}(t) = \sum_{n=1}^{2^{k-1}} \sum_{m=0}^{M-1} h_{n,m}\, \psi_{n,m}(t), \tag{11}$$

where $h_{n,m}$ denotes the Fibonacci wavelet coefficient vector and is given by

$$h_{n,m} = \left\langle g, \psi_{n,m} \right\rangle = \int_0^1 g(t) w_{n,m}(t) dt. \tag{12}$$

The matrix representation of equation (11) is expressed as

$$G = H^T \Psi(t), \tag{13}$$

where $H^T$ denotes the transpose of the vector $H$ and is of the form:

$$H = \left[ h_{1,0}, h_{1,1}, \cdots, h_{1,M-1}, h_{2,0}, h_{2,1}, \cdots, h_{2,M-1}, \cdots, h_{2^{k-1},0}, h_{2^{k-1},1}, \cdots, h_{2^{k-1},M-1} \right]^T. \tag{14}$$

The matrix $\Psi(x)$ referenced in equation (13) is the Fibonacci wavelet matrix of size $1 \times 2^{k-1}M$ defined as

$$\Psi(t) = \left[ \psi_{1,0}, \psi_{1,1}, \cdots, \psi_{1,M-1}, \psi_{2,0}, \psi_{2,1}, \cdots, \psi_{2,M-1}, \cdots, \psi_{2^{k-1},0}, \psi_{2^{k-1},1}, \cdots, \psi_{2^{k-1},M-1} \right]^T. \tag{15}$$

The following collocation points are taken into consideration for obtaining the Fibonacci wavelet approximations:

$$t_\ell = \frac{2\ell - 1}{2^k M}, \quad \ell = 1, 2, \ldots, 2^{k-1}M. \tag{16}$$

### *2.2. Operational Matrices of Integration via Fibonacci Wavelets*

In this subsection, we will construct the operational matrices of integration associated with Fibonacci wavelets (8) by following the Chen and Hsiao technique [16]:

$$\int_0^t \Psi_{n,m}(s)\, ds \cong Q\, \Psi_{n,m}(t), \tag{17}$$

where $Q$ signifies the Fibonacci wavelet operational matrix with a specific order $2^{k-1}M \times 2^{k-1}M$. For the choice $k = 2, M = 3$, we can perform integration on equation (10) at the collocation points specified in equation (16) thereby accomplishing:

$$\int_0^t \psi_{1,0}(x)\, dx = \left(0, \frac{\sqrt{3}}{6}, 0, \frac{1}{2}, 0, 0\right)^T \Psi_{6\times 6}(t),$$

$$\int_0^t \psi_{1,1}(x)\, dx = \left(-\frac{\sqrt{3}}{4}, 0, \frac{\sqrt{35}}{10}, \frac{\sqrt{3}}{4}, 0, 0\right)^T \Psi_{6\times 6}(t),$$

$$\int_0^t \psi_{1,2}(x)\, dx = \left(-\frac{29\sqrt{105}}{1680}, \frac{\sqrt{35}}{35}, \frac{1}{4}, \sqrt{\frac{5}{21}}, 0, 0\right)^T \Psi_{6\times 6}(t),$$

$$\int_0^t \psi_{2,0}(x)\, dx = \left(0, 0, 0, 0, \frac{\sqrt{3}}{6}, 0\right)^T \Psi_{6\times 6}(t),$$

$$\int_0^t \psi_{2,1}(x)\, dx = \left(0, 0, 0, -\frac{\sqrt{3}}{4}, 0, \frac{\sqrt{35}}{10}\right)^T \Psi_{6\times 6}(t),$$

$$\int_0^t \psi_{2,2}(x)\, dx = \left(0, 0, 0, -\frac{29\sqrt{105}}{1680}, \frac{\sqrt{35}}{35}, \frac{1}{4}\right)^T \Psi_{6\times 6}(t).$$

Subsequently from equation (17), we have

$$\int_0^t \Psi_{6\times1}(x)\,dx \cong Q_{6\times6}\,\Psi_6 t), \tag{18}$$

where

$$\Psi_{6\times6} = \begin{pmatrix} 0 & \frac{\sqrt{3}}{6} & 0 & \frac{1}{2} & 0 & 0 \\ -\frac{\sqrt{3}}{4} & 0 & \frac{\sqrt{35}}{10} & \frac{\sqrt{3}}{4} & 0 & 0 \\ -\frac{29\sqrt{105}}{1680} & \frac{\sqrt{35}}{35} & \frac{1}{4} & \sqrt{\frac{5}{21}} & 0 & 0 \\ 0 & 0 & 0 & 0 & \frac{\sqrt{3}}{6} & 0 \\ 0 & 0 & 0 & -\frac{\sqrt{3}}{4} & 0 & \frac{\sqrt{35}}{10} \\ 0 & 0 & 0 & -\frac{29\sqrt{105}}{1680} & \frac{\sqrt{35}}{35} & \frac{1}{4} \end{pmatrix}. \tag{19}$$

*2.3. Haar Wavelets and Function Approximation*

For any $t \in [0,1]$, the Haar wavelet family is defined by [11]:

$$h_i(t) = \begin{cases} 1, & t \in [\alpha, \beta) \\ -1, & t \in [\beta, \gamma) \\ 0, & \text{elsewhere,} \end{cases} \tag{20}$$

where

$$\alpha = \frac{k}{2^j}, \qquad \beta = \frac{k+0.5}{2^j}, \qquad \gamma = \frac{k+1}{2^j}, \tag{21}$$

$i = 0, 1, \ldots, m-1, m = 2^{p+1}, p = 0, 1, \ldots, J$ and $J$, a positive integer representing the maximum level of resolution, the parameters $j$ and $k$ denote the integer decomposition of the index $i$. Specifically, $i$ is expressed as $k + 2^j - 1$, where $0 \le j < i$, and $k$ ranges from 1 to $2^j$. Any function $g(t) \in L^2[0,1]$ can be expanded in Haar wavelet series as:

$$g(t) = b_0 h_0(x) + b_1 h_1(t) + b_2 h_2(t) + \cdots = \sum_{i=0}^{\infty} b_i h_i(t), \tag{22}$$

where $b_i, i = 0, 1, 2, \ldots$, denotes the Haar wavelet coefficients and are given by

$$b_i = \left\langle g, h_i \right\rangle = \int_0^1 g(t) h_i(t)\,dt, \tag{23}$$

If $g(t)$ is approximated as a piece-wise constant function in each sub-interval, then the infinite series given by (22) will be written in truncated series, as a result we may write the discrete form of $g(t)$ in matrix form as:

$$G = B_m^T H_m, \tag{24}$$

where $G$ and $B_m^T = [b_0(t), b_1(t), b_2(t), \cdots, b_{m-1}(t)]$ represent vectors of dimensions $1 \times m$ and $H_m$ denotes the Haar wavelet matrix of orde $m = 2^{p+1}$, defined as

$$H_m = \begin{pmatrix} h_0 \\ h_1 \\ \vdots \\ h_{m-1} \end{pmatrix} = \begin{pmatrix} h_{0,0} & h_{0,1} & \ldots & h_{0,m-1} \\ h_{1,0} & h_{1,1} & \ldots & h_{1,m-1} \\ \vdots & \vdots & \vdots & \vdots \\ h_{m-1,0} & h_{m-1,1} & \ldots & h_{m-1,m-1} \end{pmatrix}. \tag{25}$$

For obtaining the Haar wavelet approximations, the following collocation points are taken into consideration:

$$t_\ell = \frac{\ell - 0.5}{m}, \quad \ell = 1, 2, \ldots, m. \tag{26}$$

*2.4. Operational Matrices of Integration via Haar Wavelets*

Invoking the Haar wavelets as defined in (20), we construct the operational matrices of integration corresponding to Haar wavelets by following the Chen and Hsiao strategy [16]:

$$\left.\begin{aligned} SP^1_\ell(t) &= \int_0^t h_i(s)\,ds \\ P^2_\ell(t) &= \int_0^t P^1_\ell(s)\,ds \\ P^3_\ell(t) &= \int_0^t P^2_\ell(s)\,ds \end{aligned}\right\}. \tag{27}$$

By virtue of Haar wavelets (20), the integrals in (27) can be evaluated analytically. As a result, we obtain the following equations:

$$P^1_\ell(t) = \begin{cases} t - \alpha, & t \in [\alpha, \beta) \\ \gamma - t, & t \in [\beta, \gamma) \\ 0, & \text{elsewhere,} \end{cases} \tag{28}$$

$$P^2_\ell(t) = \begin{cases} 0, & t \in [0, \alpha) \\ \dfrac{1}{2}(t-\alpha)^2, & t \in [\alpha, \beta) \\ \dfrac{1}{4m^2} - \dfrac{1}{2}(\gamma - t^2), & t \in [\beta, \gamma) \\ \dfrac{1}{4m^2}, & t \in [\gamma, 1), \end{cases} \tag{29}$$

$$P^3_\ell = \begin{cases} \dfrac{1}{6}(t-\alpha)^2, & t \in [\alpha, \beta) \\ \dfrac{1}{2}(t-\beta) + \dfrac{1}{6}(\gamma - t)^3, & t \in [\beta, \gamma) \\ \dfrac{1}{4m^2}(x-\beta), & t \in [\gamma, 1) \\ 0, & \text{elsewhere.} \end{cases} \tag{30}$$

For instance, if we choose $m = 4$ and $m = 8$, respectively, then the Haar coefficient matrix $H$ and its corresponding operational matrix of integration $P$ are expressed as :

$$H_4 = \begin{pmatrix} 1 & 1 & 1 & 1 \\ 1 & 1 & -1 & -1 \\ 1 & -1 & 0 & 0 \\ 0 & 0 & 1 & -1 \end{pmatrix}, \qquad P_4 = \frac{1}{8}\begin{pmatrix} 1 & 3 & 5 & 7 \\ 1 & 3 & 3 & 1 \\ 1 & 1 & 0 & 0 \\ 0 & 0 & 1 & 1 \end{pmatrix}.$$

$$H_8 = \begin{pmatrix} 1 & 1 & 1 & 1 & 1 & 1 & 1 & 1 \\ 1 & 1 & 1 & 1 & -1 & -1 & -1 & -1 \\ 1 & 1 & -1 & -1 & 0 & 0 & 0 & 0 \\ 0 & 0 & 0 & 0 & 1 & 1 & -1 & -1 \\ 1 & -1 & 0 & 0 & 0 & 0 & 0 & 0 \\ 0 & 0 & 1 & -1 & 0 & 0 & 0 & 0 \\ 0 & 0 & 0 & 0 & 1 & -1 & 0 & 0 \\ 0 & 0 & 0 & 0 & 0 & 0 & 1 & -1 \end{pmatrix}, P_8 = \frac{1}{64} \begin{pmatrix} 32 & -16 & -8 & -8 & -4 & -4 & -4 & -4 \\ 16 & 0 & -8 & 8 & -4 & -4 & 4 & 4 \\ 4 & 4 & 0 & 0 & -4 & 4 & 0 & 0 \\ 4 & 4 & 0 & 0 & -4 & 4 & 0 & 0 \\ 1 & 4 & 2 & 0 & 0 & 0 & 0 & 0 \\ 1 & 1 & -2 & 0 & 0 & 0 & 0 & 0 \\ 1 & -1 & 0 & 2 & 0 & 0 & 0 & 0 \\ 1 & -1 & 0 & -2 & 0 & 0 & 0 & 0 \end{pmatrix}.$$

## 3. Method of Solution

In this section, we shall employ the Fibonacci wavelet method (FWM) and Haar wavelet method (HWM) for obtaining the approximate solution of the SIR epidemic model. First, we linearize the given SIR epidemic model and then we will apply both the proposed methods for obtaining the numerical solution. For solving the SIR epidemic model, it is imperative to recall the non-linear SIR model epidemic as:

$$\left.\begin{aligned} \frac{dS}{dt} &= -\alpha SI \\ \frac{dI}{dt} &= \alpha SI - \beta I \\ \frac{dR}{dt} &= \beta I \end{aligned}\right\}, \tag{31}$$

with initial conditions

$$\big(S(0), I(0), R(0)\big) = \big(S_0, I_0, R_0\big). \tag{32}$$

The linearized form of the non-linear model (31) at any general equilibrium point $(S^*, I^*, R^*)$ is given by

$$\frac{dY}{dt} = JY, \tag{33}$$

where $J$ represents the Jacobian of the model (31) at $(S^*, I^*, R^*)$ and is given by

$$J(S^*, I^*, R^*) = \begin{pmatrix} -\alpha I\Big|_{(S^*,I^*,R^*)} & -\alpha S\Big|_{(S^*,I^*,R^*)} & 0 \\ \alpha I\Big|_{(S^*,I^*,R^*)} & \big(-\alpha S - \beta\big)\Big|_{(S^*,I^*,R^*)} & 0 \\ 0 & \beta & 0 \end{pmatrix}. \tag{34}$$

Consequently, the linearized version of the non-linear model (31) at the general equilibrium point $(S^*, I^*, R^*)$ is given by

$$\left.\begin{aligned} \frac{dS}{dt} &= \big(-\alpha I\Big|_{(S^*,I^*,R^*)}\big)S - \big(\alpha S\Big|_{(S^*,I^*,R^*)}\big)I \\ \frac{dI}{dt} &= \big(\alpha I\Big|_{(S^*,I^*,R^*)}\big)S + \big(\big(-\alpha S - \beta\big)\Big|_{(S^*,I^*,R^*)}\big)I \\ \frac{dR}{dt} &= \beta I \end{aligned}\right\}. \tag{35}$$

### 3.1. Solution of SIR Epidemic Model via Fibonacci Wavelets

Approximating the highest derivatives in the model (35) in terms of Fibonacci wavelet basis as:

$$\left.\begin{aligned} \frac{dS}{dt} &= \sum_{\ell=1}^{2^{k-1}M} a_1\psi_\ell(t) \\ \frac{dI}{dt} &= \sum_{\ell=1}^{2^{k-1}M} a_2\psi_\ell(t) \\ \frac{dR}{dt} &= \sum_{\ell=1}^{2^{k-1}M} a_3\psi_\ell(t) \end{aligned}\right\}, \tag{36}$$

where $a_r = \left[h_{1,0}, h_{1,1}, \cdots, h_{1,M-1}, h_{2,0}, h_{2,1}, \cdots, h_{2,M-1}, \cdots, h_{2^{k-1},0}, h_{2^{k-1},1}, \cdots, h_{2^{k-1},M-1}\right]^T$, $r = 1, 2, 3$ are the unknown Fibonacci wavelet coefficients. Differentiating equation (36), both sides with respect to $t$ and using (32), we have

$$\left.\begin{aligned} S(t) &= S(0) + \sum_{\ell=1}^{2^{k-1}M} a_1 Q_\ell^1(t) \\ I(t) &= I(0) + \sum_{\ell=1}^{2^{k-1}M} a_2 Q_\ell^1(t) \\ R(t) &= R(0) + \sum_{\ell=1}^{2^{k-1}M} a_3 Q_\ell^1(t) \end{aligned}\right\}, \tag{37}$$

where the only unknowns are $a_1$, $a_2$ and $a_3$. Substituting (36) and (37) in equation (35), we get a system of algebraic equations. By solving the algebraic equations at the predefined collocation points (16) by Newton's method in MATLAB software, we will obtain the unknown Fibonacci wavelet coefficients $a_1$, $a_2$ and $a_3$. Thereafter, substituting $a_r$, $r = 1, 2, 3$ in equation (37), we will get the required solutions of $S(t)$, $I(t)$ and $R(t)$ via Fibonacci wavelets.

### *3.2. Solution of SIR Epidemic Model via Haar Wavelets*

Expanding the highest derivatives present in the model (35) in terms of Haar wavelet basis as:

$$\left.\begin{aligned} \frac{dS}{dt} &= \sum_{\ell=1}^{m} B_1 H_m(t) \\ \frac{dI}{dt} &= \sum_{\ell=1}^{m} B_2 H_m(t) \\ \frac{dR}{dt} &= \sum_{\ell=1}^{m} B_3 H_m(t) \end{aligned}\right\}, \tag{38}$$

where $B_r = \left[b_0(t), b_1, b_2(t) \ldots, b_{m-1}(t)\right], r = 1, 2, 3$ are the unknown Haar wavelet coefficients and $H$ is given by equation (25). Next, differentiating equation (38) both sides with respect to $t$ and using (32), we obtain

$$\left.\begin{aligned} S(t) &= S(0) + \sum_{\ell=1}^{m} B_1 P_\ell^1(t) \\ I(t) &= I(0) + \sum_{\ell=1}^{m} B_2 P_\ell^1(t) \\ R(t) &= R(0) + \sum_{\ell=1}^{m} B_3 P_\ell^1(t) \end{aligned}\right\}. \tag{39}$$

In equation (39), the only unknowns are $B_r$, $r = 1, 2, 3$. Now, by substituting (38) and (39) into (35) and taking the collocation points (26) into consideration, we obtain a system of algebraic equations. By solving the system of algebraic equations via Newton's method in MATLAB software, we will attain the values of unknown vectors $B_1$, $B_2$, and $B_3$. Next, substituting the wavelet coefficients $B_1$, $B_2$, and $B_3$ in equation (39), we will get the desired solutions $S(t)$, $I(t)$, and $R(t)$ via Haar wavelets.

## 4. Numerical Results and Discussion

In this section, we will carry out numerical simulation and analyze the behaviors of the susceptible, infected, and recovered by utilizing the operational matrices based on Fibonacci and Haar wavelets as discussed in Section 2, which converts the given model into a system of algebraic equations. The numerical simulation and behaviors of the susceptible, infected, and recovered people of the SIR epidemic model are depicted by means of Figures 2-7.

$$\left.\begin{aligned} \frac{dS}{dt} &= -0.001SI \\ \frac{dI}{dt} &= 0.001SI - 0.072I \\ \frac{dR}{dt} &= 0.072I \end{aligned}\right\}, \tag{40}$$

with initial conditions $S(0) = 620$, $I(0) = 10$ and $R(0) = 70$. From Figures 2-4, it is pertinent to mention that the numerical outcomes obtained by FWM and HWM for susceptible, infected, and recovered populations are almost identical at $K = 3, M = 4$ and $J = 3$. Figure 2 shows that the rate of susceptible population is decreasing with respect to time $t$. Figure 3 depicts that the population of the infected class is increasing with respect to time $t$. Also from Figure 4, we infer that the recovered population is increasing over time $t$. Furthermore, the results obtained $S_{FWM}(t)$ (susceptible by FWM), $I_{FWM}(t)$ (infected by FWM), $R_{FWM}(t)$ (recovered by FWM) along with $S_{HWM}(t)$ (susceptible by HWM), $I_{HWM}(t)$ (infected by HWM), and $R_{HWM}(t)$ (recovered by HWM) are almost similar.

Moreover, to show the accuracy between the proposed methods, we have computed the absolute error and relative error in Figures 5-7. The absolute error and relative error between the solutions $S_{FWM}(t)$, $I_{FWM}(t)$, $R_{FWM}(t)$ along with $S_{HWM}(t)$, $I_{HWM}(t)$, and $R_{HWM}(t)$, where the absolute error and relative error are characterized as follows:

$$AE = \left|S_{HWM} - S_{FWM}\right|, \qquad Rel(t) = \left|\frac{S_{HWM} - S_{FWM}}{S_{HWM}}\right|, \tag{41}$$

$$AE = \left|I_{HWM} - I_{FWM}\right|, \qquad Rel(t) = \left|\frac{I_{HWM} - I_{FWM}}{I_{HWM}}\right|, \tag{42}$$

$$AE = \left|R_{HWM} - R_{FWM}\right|, \qquad Rel(t) = \left|\frac{R_{HWM} - R_{FWM}}{R_{HWM}}\right|. \tag{43}$$

In addition, we have also compared the solutions of susceptible, infected, and recovered populations obtained through the Fibonacci wavelet with the Haar wavelet in tabular form. From the Tables 1-3, we conclude that both methods are close to each other.

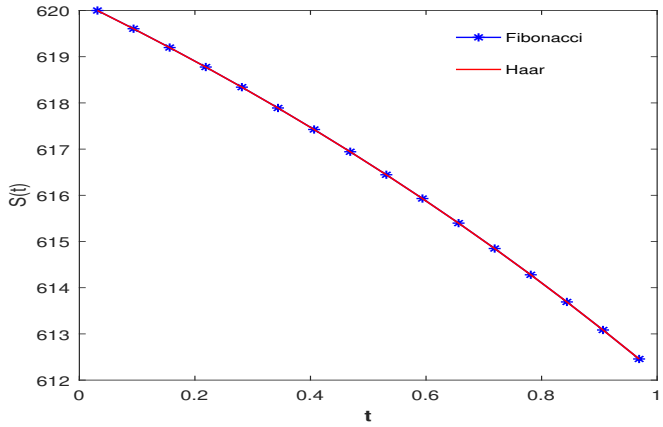


Figure 2: Plot of susceptible people at time $t$ by Fibonacci and Haar wavelets at $K = 3, M = 4$ and $J = 3$.

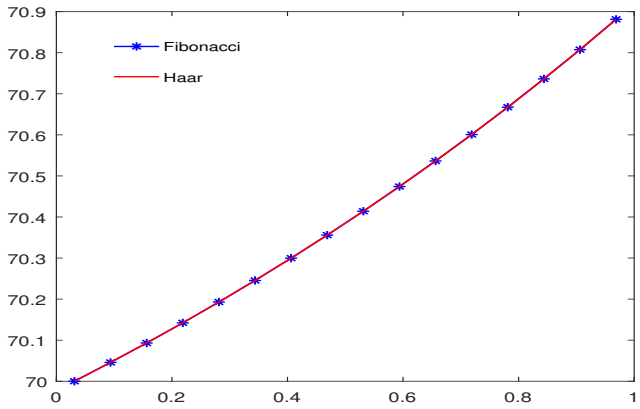


Figure 3: Plot of infected people with respect to time by Fibonacci and Haar wavelets at $K = 3, M = 4$ and $J = 3$.

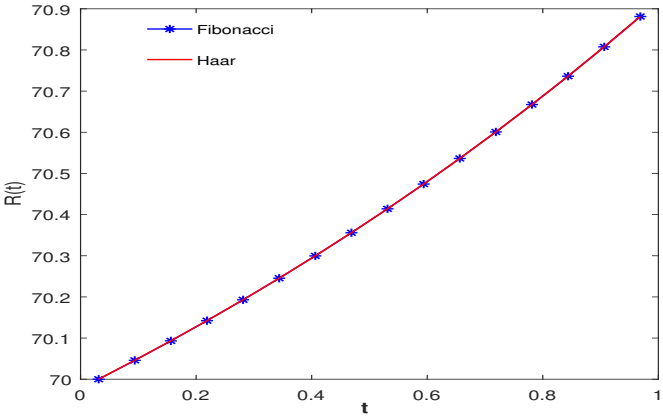


Figure 4: Plot of recovered people at time $t$ by Fibonacci and Haar wavelets at $K = 3, M = 4$ and $J = 3$.

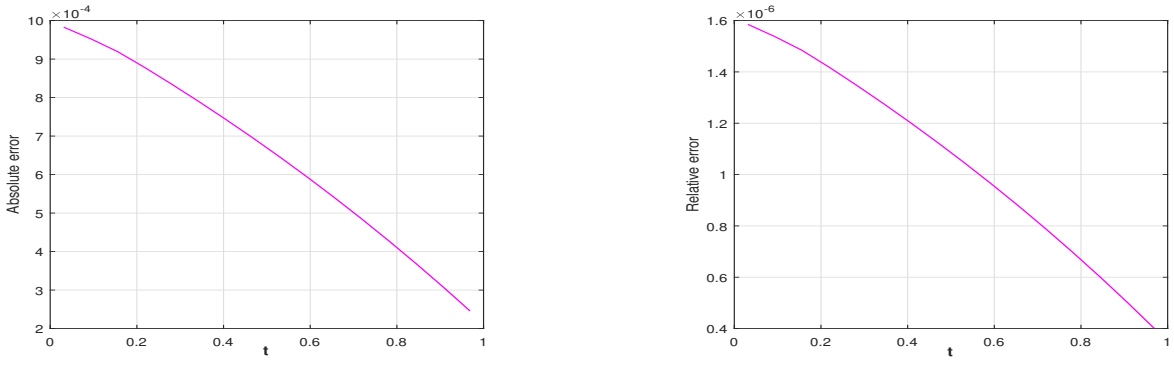


(*a*) (*b*)

Figure 5: Relative and absolute error between FWM and HWM for the class $S(t)$.

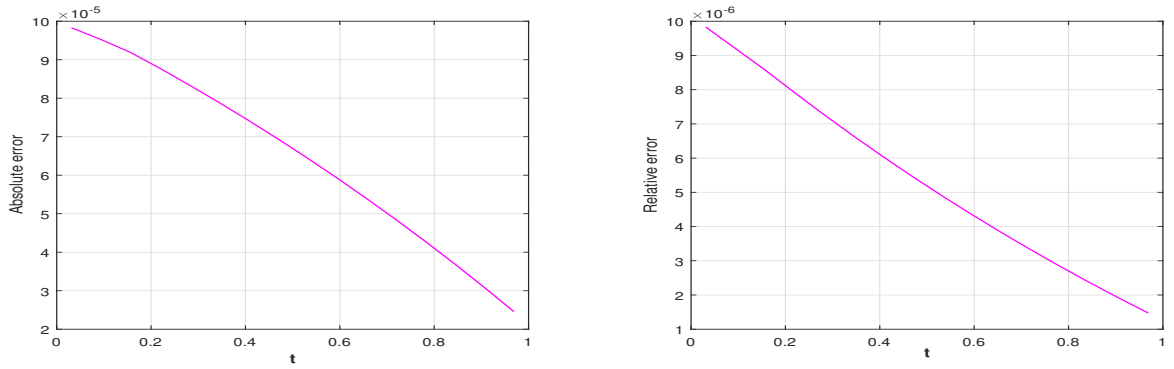


(*a*) (*b*)

Figure 6: Comparison of relative error and absolute between FWM and HWM for the class $I(t)$ .

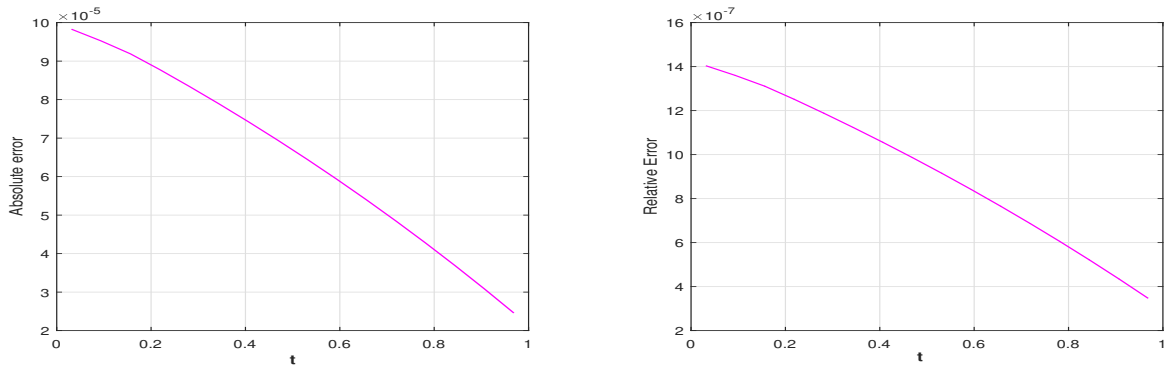


(*a*) (*b*)

Figure 7: comparison of the relative error and absolute error between proposed methods for the class $R(t)$.

| t ↓ | FWM | RK4[20] | RPS[20] |
|---|---|---|---|
| 0.1 | 619.3630333045 | 619.3630315796 | 619.3630315791 |
| 0.2 | 618.6909398455 | 618.6909370609 | 618.6909370597 |
| 0.3 | 617.9818662901 | 617.9818692109 | 617.9818692025 |
| 0.4 | 617.2338998682 | 617.2338939798 | 617.2338939757 |
| 0.5 | 616.4449824427 | 616.4449876950 | 616.4449876822 |
| 0.6 | 615.6130332236 | 615.6130341588 | 615.6130341421 |
| 0.7 | 614.7358218885 | 614.7358219653 | 614.73582195284 |
| 0.8 | 613.8110448211 | 613.8110418712 | 613.8110418536 |
| 0.9 | 612.8362800988 | 612.8362842538 | 612.836284225 |

Table 1: Comparison of FWM with the $RK4$ and $RPS$ for susceptible at $K = 3, M = 4$.

| t ↓ | FWM | RK4[20] | RPS[20] |
|---|---|---|---|
| 0.1 | 10.5629569164 | 10.5629598705 | 10.5629598709 |
| 0.2 | 11.1568891861 | 11.1568820133 | 11.1568820144 |
| 0.3 | 11.7833841048 | 11.7833849513 | 11.7833849586 |
| 0.4 | 12.4441608259 | 12.4441620994 | 12.4441621031 |
| 0.5 | 13.1409856662 | 13.1409840323 | 13.1409840435 |
| 0.6 | 13.8757021034 | 13.8757008108 | 13.8757008253 |
| 0.7 | 14.6502449588 | 14.6502440931 | 14.6502441041 |
| 0.8 | 15.4666220146 | 15.4666291698 | 15.4666291853 |
| 0.9 | 16.3269598710 | 16.3269568911 | 16.3269569155 |

Table 2: Comparison of FWM with the $RK4$ and $RPS$ for infected individual at $K = 3, M = 4$.

| t ↓ | FWM | RK4[20] | RPS[20] |
|---|---|---|---|
| 0.1 | 70.0740088587 | 70.0740085497 | 70.0740085498 |
| 0.2 | 70.1521889611 | 70.1521809256 | 70.1521809257 |
| 0.3 | 70.2347439430 | 70.2347458376 | 70.2347458387 |
| 0.4 | 70.3219450324 | 70.3219439206 | 70.3219439211 |
| 0.5 | 70.4140292273 | 70.4140282725 | 70.4140282742 |
| 0.6 | 70.5112639211 | 70.5125663085 | 70.5112650324 |
| 0.7 | 70.6139358387 | 70.613933941 | 70.6139339429 |
| 0.8 | 70.7223209258 | 70.7223289588 | 70.7223289610 |
| 0.9 | 70.8367585498 | 70.8367588550 | 70.8367588586 |

Table 3: Comparison of the solutions acquired via FWM for the recovered class with $RK4$ and $RPS$ at $K = 3, M = 4$.

## 5. Conclusion

In the present article, we developed a new wavelet-based numerical technique involving the Fibonacci wavelets to solve the SIR epidemic model, which is governed by a system of non-linear first order differential equations. The operational matrix based on the Fibonacci wavelets are employed to convert the SIR epidemic model into a system of algebraic equations. The system of algebraic equations can be solved by different numerical techniques, including Newton's method, Broyden's method, *fsolve* command in MATLAB, and many more. The behaviors of susceptible, infected and recovered populations are also illustrated graphically. The obtained results are compared with the Haar wavelet method to show the accuracy and efficacy of the Fibonacci wavelet method. The numerical simulations suggests that both the methods are very close to each other, thus verifying the authenticity of the Fibonacci wavelet-based collocation method.

*Conflict of interests:*

The authors declare that they have no conflict of interest.

## References


[1] G-Parra, G., Arenas, A.J., Charpentier, B.M.C.: Combination of nonstandard schemes and Richardson's extrapolation to improve the numerical solution of population models, Math. Comput. Model. **52**, 1030-1036 (2010)

[2] Kanyiri, C.W., Mark, K., Luboobi, L.: Mathematical analysis of influenza A dynamics in the emergence of drug resistance, Comput. Math. Methods Med. **2018**, 2434560 (2018)

[3] Baleanu, D., Mohammadi, H., Rezapour, S.: A mathematical theoretical study of a particular system of Caputo-Fabrizio fractional differential equations for the Rubella disease model, Adv. Differ. Equ. **(184)**, https://doi.org/10.1186/s13662-020-02614-z (2020)

[4] Qureshi, S., Jan, R.: Modeling of measles epidemic with optimized fractional order under Caputo differential operator, Chaos Solit. Fractals. **145**, 110766 (2021)

[5] Zafar, Z.U.A., Zaib, S., Hussain, M.T., Tunç, Javeed, S.: Analysis and numerical simulation of tuberculosis model using different fractional derivatives, Chaos Solit. Fractals. **160**, 112202 (2022)

[6] Kermack, W.O., McKendrick, A.G.: A contribution to the mathematical theory of epidemics. Proc. R. Soc. Lond. Ser. A. **115**(772), 700-721 (1927)

[7] Ferguson, N.M., Keeling, M.J., Edmunds, W.J., Gani, R., Grenfell, B.T., Anderson, R.M., Leach, S.: Planning for smallpox outbreaks, Nature **425**, 681-685 (2003)

[8] Stilianakis, N.I., Perelson, A.S., Hayden, F.G.: Emergence of drug resistance during an influenza epidemic: Insights from a mathematical model, J. Infect. Dis. **177**, 863-873 (1998)

[9] Chaharborj, S., Bakar, M., Fudziah, I., Akma, I., Malik, A., Alli, V.: Behavior stability in two SIR-style models for HIV, Int. J. Math. Anal. **4**, 427-434 (2010)

[10] Debnath, L., Shah, F.A.; *Wavelet Transforms and Their Applications*, Birkhäuser, New York, (2015)

[11] Lepik, U., Hein, H.: *Haar Wavelets with Applications*, Springer, New York, (2014)

[12] Shah, F.A., Irfan, M. , Nisar, K.S., Matoog, R.T., Mahmoud, E.E.: Fibonacci wavelet method for solving time-fractional telegraph equations with Dirichlet boundary conditions, Result. Phys. **24**, 104-123 (2021).

[13] Shah, F.A., Irfan, Generalized wavelet method for solving fractional bioheat transfer model during hyperthermia treatment, Int. J. Wavelets Multiresolut. Inf. Process. **19**, 2050090 (2021)

[14] Srivastava, H.M., Irfan, M., Shah, F.A.: A Fibonacci Wavelet method for solving dual-phase-lag heat transfer model in multi-layer skin tissue during hyperthermia treatment, Energies. **14(8)**, 2254 (2021)

[15] Irfan, M., Shah, F.A., Nisar, K.S.: Gegenbauer wavelet quasi-linearization method for solving fractional population growth model in a closed system, Math. Methods. Appl. Sci. https://doi.org/10.1002/mma.8006 (2021)

[16] Chen C.F.,Hsiao, C.H.: Haar wavelet method for solving lumped and distributed-parameter systems, IEE Proc. Control Theory Appl. **144**, 87-94 (1997)

[17] Shah,F.A., Tantary, A.Y.: *Wavelet Transforms: Kith and Kin (1st ed.)*, Chapman and Hall/CRC, https://doi.org/10.1201/9781003175766

[18] Falcon, S., Plaza, A.: On *k*-Fibonacci sequences and polynomials and their derivatives, Chaos Soliton Fract. **39**, 1005-1019 (2009)

[19] Sabermahani, S., Ordokhani, Y., Yousefi, S.A.: Fibonacci wavelets and their applications for solving two classes of time-varying delay problems, Optim. Control Appl. Meth. **41**, 395-416 (2019)

[20] Hasan, S., Al-Zoubi, A., Freihet, A., Al-Smadi, M., Momani, S.: Solution of fractional SIR epidemic model using residual power series method, Appl. Math. **13**, 13, 1-9 (2019)